Electronic structure of tetragonal $BaK_{2-x}Ba_xBi_2O_7$ and related layer-type bismuthates

L. F. Mattheiss
AT&T Bell Laboratories, Murray Hill, New Jersey 07974
(Received 21 November 1991)

The electronic structure of body-centered-tetragonal $BaK_2Bi_2O_7$, an ordered prototype of the recently synthesized perovskite-type layer compound $BaK_{1.3}Ba_{0.7}Bi_2O_7$, has been calculated with the use of the linear augmented-plane-wave method. In rigid-band terms, the results predict metallic properties for the entire $BaK_{2-x}Ba_xBi_2O_7$ alloy series, with $E_F(x)$ rising with increasing x to gradually fill a pair of nearly two-dimensional $(sp\sigma)^*$ conduction bands. For compositions $x>0.8$, the onset for filling the upper $(sp\sigma)^*$ subband produces a sharp increase in the density of states. The resulting value (per Bi) is about 50% greater than that for cubic $Ba_{1-y}K_yBiO_3$ near the composition ($y\approx 0.3$–0.4) where T_c (~ 30 K) is a maximum. This suggests that a slightly increased Ba composition ($x\sim 0.8$) should provide more favorable conditions for possible superconductivity in these $BaK_{2-x}Ba_xBi_2O_7$ alloys than those predicted for the nonsuperconducting $x\sim 0.7$ phase that has been prepared thus far.

Since the discovery[1] of high-temperature superconductivity in the cubic $Ba_{1-x}K_xBiO_3$ alloy system, with measured T_c's that have reached the 30 K range,[2] efforts to synthesize new bismuthate and plumbate superconducting phases have been largely unsuccessful.[3–9] The sole exception has been the observation of superconductivity ($T_c\approx 3.5$ K) in the cubic $BaPb_{1-x}Sb_xO_3$ alloy system[4] with $x\approx 0.25$. This transition temperature is significantly lower than the value ($T_c\approx 12$ K) that was observed initially by Sleight, Gillson, and Bierstedt[10] in the nearly-cubic $BaPb_{1-x}Bi_xO_3$ system in the same composition range, $x\approx 0.25$–0.30. This suggests that the increased Bi(6s) binding energy relative to the Pb(6s) and Sb(5s) values may play an important role in enhancing the superconducting properties of the Bi-based compounds.

In their work on the Ba-Pb-O and Ba-Pb-Bi-O systems, Fu *et al.*[5] discovered that these materials form a Ruddlesden-Popper-type[11] homologous alloy series with general composition $Ba_{n+1}(Pb_{1-x}Bi_x)_nO_{3n+1}$. These tetragonal phases consist of n perovskite-type $BaPb_{1-x}Bi_xO_3$ layers, which are separated along the c axis by rocksalt-type BaO bilayers. The $n=1$ and $n=\infty$ end members of this series correspond to body-centered-tetragonal (bct) $Ba_2Pb_{1-x}Bi_xO_4$ and (nearly) cubic $BaPb_{1-x}Bi_xO_3$, respectively. The former compound shares the same K_2NiF_4-type structure with the high-T_c cuprate superconductor $La_{2-x}Ba_xCuO_4$ (Ref. 12). Thus, these Ruddlesden-Popper phases provide an interesting structural link between the cubic bismuthate high-T_c superconductors and their tetragonal cuprate counterparts. They also provide a valuable system for investigating the influence of dimensionality on the superconducting properties of chemically similar two- and three-dimensional perovskite-type phases.

Initial efforts to induce metallic behavior and superconductivity in these Pb-based tetragonal Ruddlesden-Popper phases via Bi→Pb substitutional doping have been unsuccessful.[6,7,9] One problem with this approach is that it ignores the successful strategy[1] of leaving the conducting Pb-O or Bi-O octahedral complexes intact and instead doping substitutionally at the chemically and electronically inactive Ba sites. However, Cava *et al.*[13] have recently synthesized a very promising material in this regard, a K-doped, Bi-based $n=2$ member of the Ruddlesden-Popper series with general formula $BaK_{2-x}Ba_xBi_2O_7$ and composition $x\approx 0.7$. While superconductivity has not been observed in these samples, a simple rigid-band extrapolation of previous band-structure results for the isostructural $Ba_{n+1}Pb_nO_{3n+1}$ series[14] suggests that a slightly increased Ba composition ($x\geq 0.8$) should produce more favorable conditions for possible superconductivity in these materials.

In order to address these issues, a scalar-relativistic version[15] of the linear augmented-plane-wave (LAPW) method has been applied to calculate the electronic band properties of $BaK_2Bi_2O_7$ and related layered bismuthates (including Ba_2BiO_4 and $Ba_3Bi_2O_7$). The $BaK_2Bi_2O_7$ and $Ba_3Bi_2O_7$ results represent the ordered end-member prototypes of the $BaK_{2-x}Ba_xBi_2O_7$ alloy series that has been synthesized[13] thus far only with the composition $x\approx 0.7$. These end-member band-structure results confirm the validity of a rigid-band treatment for intermediate doping compositions x. They also confirm that doping at the electronically and chemically inactive Ba site in the cubic $Ba_{1-x}K_xBiO_3$ alloys[1,16,17] should also be effective here.

The present LAPW calculations have been carried out self-consistently in the local-density approximation with the use of the Wigner interpolation formula[18] to treat exchange and correlation effects. The implementation[15] imposes no shape approximations on either the crystalline charge density or potential. In this investigation, the LAPW basis has included plane waves with a 10.5-Ry cutoff (~ 770 LAPW's) and spherical-harmonic terms through $l=8$ within the muffin-tin spheres. The potential and charge density have been expanded using ~ 9200 plane waves in the interstitial region and lattice-harmonic expansions ($l_{max}=6$) inside the muffin-tin spheres. Brillouin-zone integrations have been carried out using a

ten-**k**-point sample in the $\frac{1}{16}$ irreducible Brillouin-zone wedge. The atomic Ba($5p^6 6s^2$), K($3p^6 4s$), Bi($6s^2 6p^3$), and O($2s^2 2p^4$) states are treated as valence electrons, while a frozen-core approximation is applied to the more tightly bound core levels.

The essential features of the $BaK_{2-x}Ba_xBi_2O_7$ structure are illustrated in Fig. 1. The primitive cell contains two perovskite-type layers with equivalent Bi sites that are octahedrally coordinated by oxygens. The $BaK_{1.3}Ba_{0.7}Bi_2O_7$ structural parameters, which have been determined by single-crystal x-ray-diffraction measurements,[13] are summarized in Table I. According to these structural parameters, the Bi-O coordination geometry is quite symmetrical. In particular, the Bi-O bond distances (~2.14 Å) with the planar [O(2)] oxygens are slightly larger than the average apical-oxygen [~2.17 Å for O(1) and ~2.04 Å for O(3)] values. A similar anisotropy occurs in Ba_2PbO_4, where the Pb coordination geometry involves two short (~2.06 Å) apical Pb-O bond distances and four longer (~2.14-Å) planar values.[14]

An interesting aspect of these x-ray structural data is the fact that they reveal a preference between the two Ba sites (types 2b and 4e, respectively) in regard to K→Ba substitution. In particular, the data analysis shows that the type-2b sites are occupied entirely by Ba atoms and the K-Ba alloying effects are confined solely to the type 4e sites. These form the rocksalt-type bilayers that separate neighboring cells along the *c* direction.

The present LAPW band-structure results for the ordered $BaK_2Bi_2O_7$ alloy in which these 4e sites are fully occupied by K atoms are shown in Fig. 2. The 23-band valence- and conduction-band manifold, which extends from ~+4 to −11 eV, evolves from the O(2*p*) and Bi(6*s*) states. The Fermi level occurs within the lower portion of a pair of $(sp\sigma)^*$ antibonding subbands that originate from the strong Bi-O nearest-neighbor interactions. Their bonding counterparts intersect the corelike bands at lower energies (~−10.0 and −10.5 eV), which represent the Ba(5*p*) and K(3*p*) levels, respectively. Since the lowest Ba and K conduction bands are located well above (~5 eV) the $BaK_2Bi_2O_7$ Fermi level, these constituents essentially donate their three outer ($6s^2$ and 4*s*) electrons to the Bi(6*s*)-O(2*p*) band manifold.

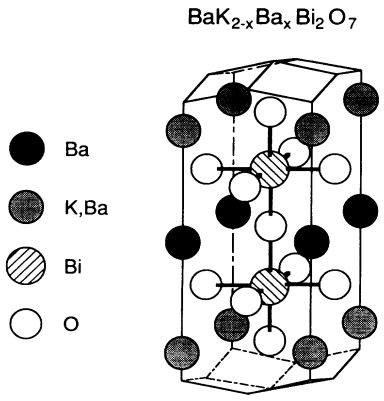

FIG. 1. Primitive body-centered-tetragonal unit cell for $BaK_{2-x}Ba_xBi_2O_7$. Oxygens in the Ba, Bi, and K-Ba planes are denoted O(1), O(2), and O(3), respectively.

TABLE I. Measured (Ref. 13) atom-position parameters for the body-centered-tetragonal compound $BaK_{1.3}Ba_{0.7}Bi_2O_7$ with space group $I4/mmm$ (D_{4h}^{17}) and lattice-parameter values $a = 4.2477$ Å and $c = 21.885$ Å.

Atom	Type	*x*	*y*	*z*
Ba	2b	$\frac{1}{2}$	$\frac{1}{2}$	0
$K_{1.3}Ba_{0.7}$	4e	$\frac{1}{2}$	$\frac{1}{2}$	0.189 23
Bi	4e	0	0	0.099 34
O(1)	2a	0	0	0
O(2)	8g	$\frac{1}{2}$	0	0.091 4
O(3)	4e	0	0	0.192 3

The $(sp\sigma)^*$ conduction bands are very similar to those obtained previously [see Fig. 5(a) of Ref. 14] from a tight-binding treatment for the isostructural and isoelectronic compound $Ba_3Pb_2O_7$, where tight-binding parameters have been derived from a fit to LAPW results for Ba_2PbO_4. According to this tight-binding analysis,[14] the splitting between the two $(sp\sigma)^*$ conduction bands in Fig. 2 originates from the fact that the upper $(sp\sigma)^*$ band, which is odd under reflection in the basal plane, interacts with two apical oxygens whereas the lower (even) $(sp\sigma)^*$ band interacts only with one. As expected, the main

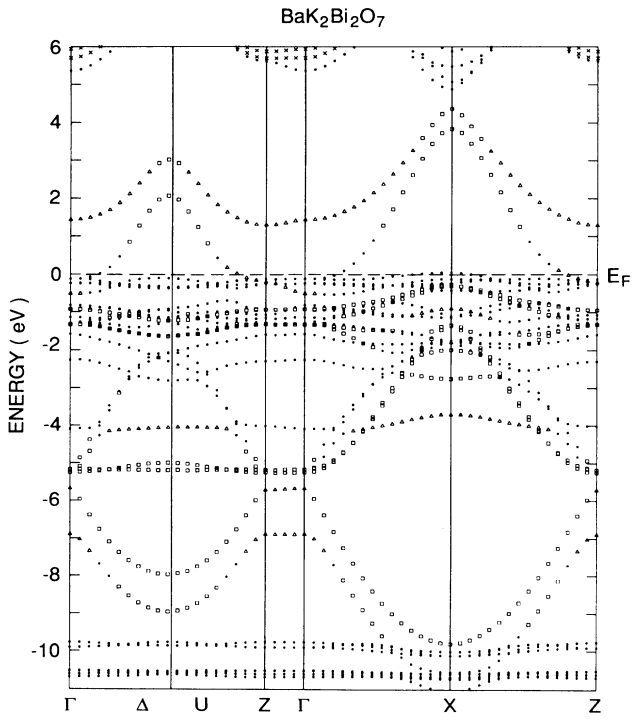

FIG. 2. LAPW band results for $BaK_2Bi_2O_7$ along symmetry lines in the bct Brillouin zone. Those bands labeled by squares [triangles] have at least 40% Bi(6*s*)-O((2)$p(x,y)$) [Bi(6*s*)-O((1,3)$p(z)$)] orbital weight within the corresponding muffin-tin spheres. The x's identify bands with significant (>30%) Ba or K *d*-type character.

difference in the present $BaK_2Bi_2O_7$ bands is due to the increased binding energy ($\sim$2.4 eV) of the atomic Bi(6*s*) level relative to that of the corresponding Pb(6*s*) state. In contrast to the calculated semiconducting behavior in $Ba_3Pb_2O_7$, this shifts the $BaK_2Bi_2O_7$ $(sp\sigma)^*$ bands to lower energies to the extent that they overlap the nonbonding O(2*p*) bands and produce metallic behavior. A less obvious consequence of the increased Bi(6*s*) binding energy is to increase the O(2*p*) component of the conduction-electron states near E_F. Qualitatively, this could increase T_c by enhancing the coupling between the Fermi-surface electrons and bond-stretching oxygen phonons.

As shown by the square and triangle symbols, the orbital character of the $(sp\sigma)^*$ subbands varies systematically with wave vector and energy. The lower-energy portions of each subband involve primarily Bi(6*s*) $(sp\sigma)$ interactions with apical oxygen [O(1) and O(3), respectively] $p(z)$-type orbitals, while the uppermost states exhibit planar Bi(6*s*)-O(2) $p(x,y)$ character. As discussed previously,[14] this variation from apical-to-planar Bi-O bonding effects in the $BaK_2Bi_2O_7$ $(sp\sigma)^*$ conduction bands is a manifestation of their hybrid nature.

The band-structure results in Fig. 2 exhibit nearly two-dimensional (2D) characteristics, despite the basic isotropic character of the central Bi(6*s*) states. These 2D features result from the rocksalt-type K_2O_2 double-layers, which act as insulating barriers to separate neighboring $BaBi_2O_5$ units along the *c* axis. One obvious measure of 2D behavior is the limited dispersion exhibited by the bands along the ΓZ direction. Another is the symmetry of the bands about X and the midpoint of the ΔU line. These lines, which are coplanar in an extended-zone scheme, are separated vertically by the same ΓZ dimension $(2\pi/c)$ in the primitive Brillouin zone.

These 2D band characteristics originate from the fact that the continuity of the O(3)-Bi-O(1)-Bi-O(3) *c*-axis bonds in Fig. 1 is interrupted by the body-centering translation, which places the electronically inactive K^+ ions above and below the O(3) sites in neighboring cells. As a result, the strong apical-oxygen $(sp\sigma)$ interactions with the intermediate Bi atoms produce pairs of bonding and antibonding molecular-orbital-type states that are shifted by large energies but in turn exhibit minimal *c*-axis dispersion.[14]

This qualitative picture is reflected by the valence-electron charge-density results that are shown in Fig. 3. The strong nearest-neighbor Bi-O $(sp\sigma)$ bonds are identified by the long-dashed curves that represent the 0.04-electron/(a.u.)^3 contours. The bonding is nearly isotropic about the Bi site.[19] The planar Bi-O(2) $(sp\sigma)$ bonds extend periodically throughout the crystal along the [100] and [010] directions. However, the corresponding apical-oxygen [O(3)] bond charge is visibly confined, diminishing rapidly in the upper portion of the figure rather than continuing in the direction of the neighboring K^+ ion (at a distance of $\sim$2.59 Å) in the adjoining layer.

The $BaK_2Bi_2O_7$ density-of-states $[N(E)]$ results in Fig. 4 provide a general overview of the electronic properties for this compound. These results have been calculated using tetrahedral interpolation, based on LAPW results

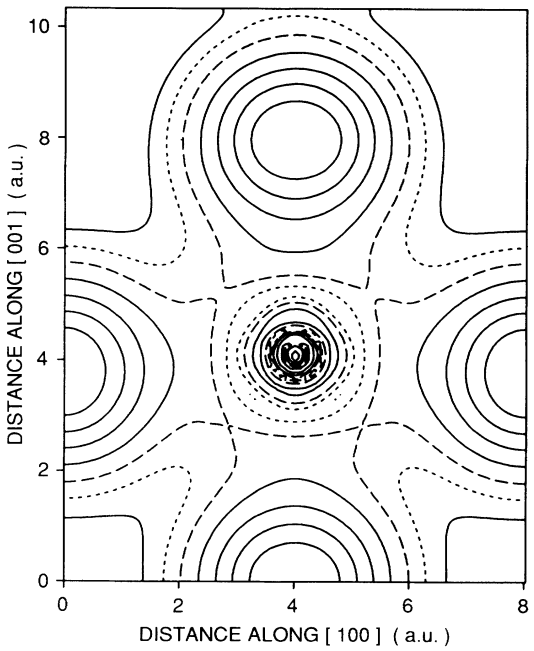

FIG. 3. Valence-electron charge-density contours on a central (100) plane of $BaK_2Bi_2O_7$. The lower boundary is the basal reflection plane that contains the O(1) atoms. Neighboring layers contain Bi-O(2) and O(3) sites, respectively. The charge densities are expressed in units of electrons/(a.u.)^3 and adjacent contours increase by a factor of 2. The 0.02 and 0.04 contours are identified by the short and long dashes, respectively.

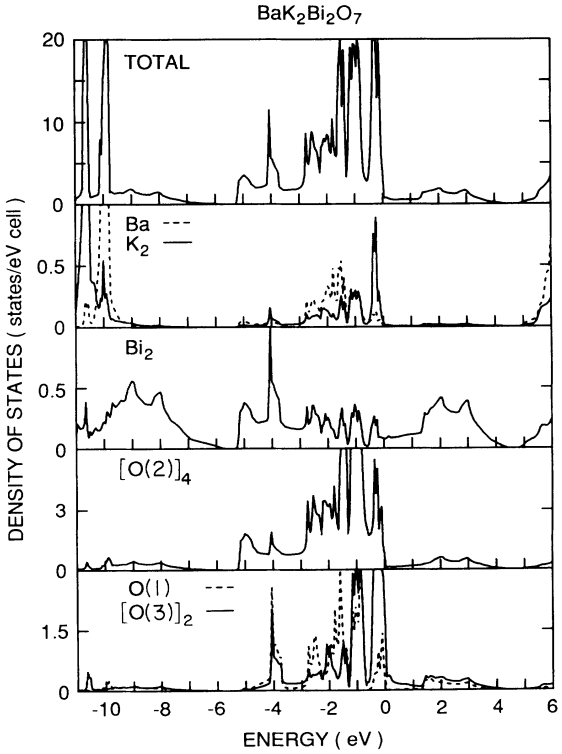

FIG. 4. Total and muffin-tin projected density-of-states results for $BaK_2Bi_2O_7$.

at 42 uniformly distributed **k** points in the $\frac{1}{16}$ irreducible Brillouin-zone wedge. The $BaK_2Bi_2O_7$ Fermi level falls on the leading edge of a $N(E)$ peak that arises primarily from the weakly bonding $p(x,y)$ states at the O(3) sites that are clustered near E_F in Fig. 2. As discussed in more detail below, Ba→K substitution will raise the Fermi level and decrease $N(E_F)$ from the undoped value (~3.7 states/eV cell) to a more typical value (~0.5 states/eV cell) for the $(sp\sigma)^*$ conduction band.

As expected from earlier studies on related tetragonal[14] (Ba_2PbO_4) and nearly-cubic[17] ($BaBiO_3$ and $Ba_{0.5}K_{0.5}BiO_3$) phases, the muffin-tin projected Ba and K components are extremely small in the $(sp\sigma)^*$ conduction-band energy range. Thus, these electronically inactive divalent or monovalent constituents are ideal candidates for raising the Fermi level via substitutional doping while minimizing disorder-induced scattering of the conduction electrons near E_F. As Cava *et al.*[13] have shown, Ba→K substitution leads to one interesting possibility, $BaK_{2-x}Ba_xBi_2O_7$. Clearly, other possible divalent constituents (e.g., $BaK_{2-x}Sr_xBi_2O_7$, etc.) should also be explored.

As in the cubic $Ba_{1-x}K_xBiO_3$ system,[1,17] the doping strategy in the alkali-doped bct $Ba_{n+1}Bi_nO_{3n+1}$ homologous series is to lower E_F within the $(sp\sigma)^*$ conduction band(s) in order to stabilize the target bct phase. Though the evidence is limited, there are indications that the tetragonal $Ba_{n+1}Bi_nO_{3n+1}$ compounds may be unstable in the small-n limit. For example, efforts to synthesize the undoped $n=1$ bct phase, Ba_2BiO_4, have been unsuccessful thus far.[6,9,20,21] Instead of the desired tetragonal phase, these studies have shown that, near the 2:1:4 composition range, the Ba-Bi-O system forms an oxygen-deficient face-centered-cubic perovskite[20,21] in which Bi occupies one octahedral site, while a $Bi_{1-x}Ba_x$ mixture occupies the other.

In the case of $BaK_{1.3}Ba_{0.7}Bi_2O_7$, Cava *et al.*[13] have noted that they were unable to synthesize this tetragonal $n=2$ Ruddlesden-Popper-type phase through the application of conventional ceramic-processing methods. Instead, it was obtained only through the use of an electrochemical growth technique. X-ray-diffraction evidence indicated that the composition of the electrochemically-deposited phase could not be changed significantly from the value $x \approx 0.7$ by variations in the preparation conditions. Clearly, these alternative processing methods should also be explored in efforts to produce the alkali-doped $n=1$ Ruddlesden-Popper phase, $Ba_{2-x}K_xBiO_4$. One very promising approach involves the use of molecular-beam epitaxy, a technique that has been applied successfully to grow superconducting cubic $Ba_{1-x}Rb_xBiO_3$ and $Ba_{1-x}K_xBiO_3$ thin films.[22] This technique may provide a valuable alternative for producing K-doped $Ba_{2-x}K_xBiO_4$ or Ba-enriched $BaK_{2-x}Ba_xBi_2O_7$ bct-phase samples.

Despite their possibly unstable nature, it is interesting to investigate the electronic structure of the undoped Ba_2BiO_4 and end-member $Ba_3Bi_2O_7$ compounds. An approximate structure for the 2:1:4 bct phase has been derived from the $BaK_{1.3}Ba_{0.7}Bi_2O_7$ structural data of Table I. These estimated parameters for Ba_2BiO_4 include the values $a=4.25$ Å, $c=13.19$ Å, $z(\text{Ba})=0.149$, and $z(\text{O})=0.154$. These values are in reasonable agreement with the corresponding Ba_2PbO_4 parameters[23] [$a=4.30$ Å, $c=13.3$ Å, $z(\text{Ba})=0.145$, and $z(\text{O})=0.155$]. For the $Ba_3Bi_2O_7$ calculations, the $BaK_{1.3}Ba_{0.7}Bi_2O_7$ structural

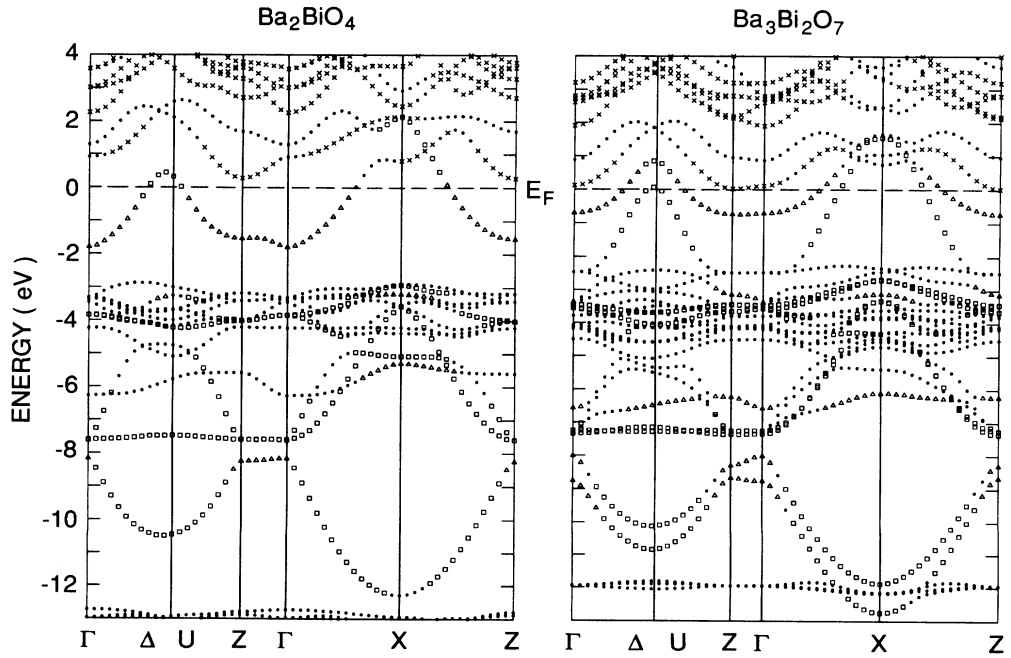

FIG. 5. LAPW energy-band results for the undoped $n=1$ (Ba_2BiO_4) and $n=2$ ($Ba_3Bi_2O_7$) members of the $Ba_{n+1}Bi_nO_{3n+1}$ homologous series. Bands with specific orbital character are labeled in accordance with Fig. 2.

parameters of Table I have been used directly.

The results of LAPW calculations for these bct forms of Ba_2BiO_4 and $Ba_3Bi_2O_7$ are shown in Fig. 5. In these materials, the Fermi level is raised so that the $(sp\sigma)^*$ band(s) is half filled. Overall, the Ba_2BiO_4 bands are extremely similar to the earlier Ba_2PbO_4 results,[14] although the increased Bi(6*s*) binding energy has reduced the calculated 1.7 eV semiconductor gap in Ba_2PbO_4 to a 1.1-eV gap separating the lowest $(sp\sigma)^*$ state at Γ and the top of the nonbonding O(2*p*) manifold at X. The lower portions of the Ba(5*d*) bands lie slightly above E_F and intersect the $(sp\sigma)^*$ band near X, in a manner similar to the Ba_2PbO_4 results.

Below E_F, the $Ba_3Bi_2O_7$ results in Fig. 5 are in good qualitative agreement with the corresponding $BaK_2Bi_2O_7$ bands of Fig. 2. The main changes occur above E_F, where the Ba(5*d*) bands have dropped in energy to the point where they nearly intersect the Fermi level. This could be a partial consequence of neglecting alloying-induced changes in the assumed structure for the $BaK_{2-x}Ba_xBi_2O_7$ system. Nevertheless, the close similarities between the $BaK_2Bi_2O_7$ (Fig. 2) and $Ba_3Bi_2O_7$ (Fig. 5) conduction-band results provides strong justification for the rigid-band treatment of the intermediate $BaK_{2-x}Ba_xBi_2O_7$ alloys.

An expanded plot of the $(sp\sigma)^*$ conduction bands and the corresponding density of states for this system, as derived from the $BaK_2Bi_2O_7$ results, is shown in Fig. 6. The interior scale presents the rigid-band variation of $E_F(x)$ with doping in the $BaK_{2-x}Ba_xBi_2O_7$ alloys. As indicated, $N(E,x)$ decreases rapidly for $x>0$ and then increases quite gradually to the value 0.53 states/eV cell (or 0.27 states/eV Bi) for $x=0.7$, the composition of the nonsuperconducting electrochemically-prepared material.[13] For purposes of comparison, the corresponding rigid-band density-of-states values[17] for the cubic $Ba_{1-x}K_xBiO_3$, compounds near the maximum-T_c composition $x\approx 0.3-0.4$ are in the range 0.46–0.52 states/eV Bi. Thus, the failure to observe superconductivity in $BaK_{1.3}Ba_{0.7}Bi_2O_7$ may be due in part to the reduced value of $N(E_F)$ for the bct versus the cubic phase.

As discussed previously,[14] there are also geometrical factors that favor an enhanced electron-phonon coupling in the cubic phase relative to its tetragonal counterparts. Namely, an analysis based on a simple tight-binding model[16] shows that the electron-phonon-coupling strength of the cubic $(sp\sigma)^*$ band is focused strongly near half filling and is enhanced by the fact that there are a larger number (i.e., 6 vs 4) of face-shared oxygen neighbors. The corresponding coupling in the bct compounds is more diffuse; while the face-sharing oxygen contributions remain at half filling, the corresponding apical-oxygen interactions are concentrated near the $(sp\sigma)^*$ conduction-band edges.

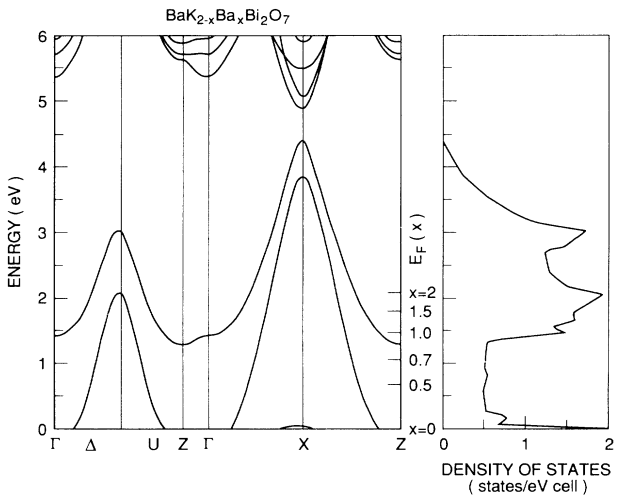

FIG. 6. Calculated variation of the $BaK_{2-x}Ba_xBi_2O_7$ Fermi level $E_F(x)$ with x within the $(sp\sigma)^*$ conduction bands according to a rigid-band treatment.

According to the results in Fig. 6, this suggests that $BaK_{2-x}Ba_xBi_2O_7$ alloys with an increased Ba content $x\geq 1$ should provide more favorable band properties for possible superconductivity. Not only is the density of states increased significantly (~0.7–0.8 states /eV Bi), but the electron-phonon-coupling strength should also be enhanced by the added contribution from the apical oxygens.

To summarize, the electronic band properties of the $n=1$ and $n=2$ members of the bct Ruddlesden-Popper homologous series have been calculated and analyzed, with particular emphasis on the $n=2$ alloy, $BaK_{2-x}Ba_xBi_2O_7$. A rigid-band treatment of this phase, based on LAPW results for the end-member compounds $BaK_2Bi_2O_7$ and $Ba_3Bi_2O_7$, suggests that an increased Ba concentration ($x\geq 1$) should provide band properties near E_F that are more favorable for superconductivity than the $x\approx 0.7$ ($BaK_{1.3}Ba_{0.7}Bi_2O_7$) composition that has been prepared electrochemically and found not to superconduct. The results also suggest that the single-layer K-doped $Ba_{2-x}K_xBiO_4$ bct phase is an equally promising high-T_c candidate.

ACKNOWLEDGMENTS

I am pleased to thank my colleagues R. J. Cava, E. H. Hartford, E. S. Hellman, and T. Siegrist for several valuable discussions on the subject of this investigation.

[1]L. F. Mattheiss, E. M. Gyorgy, and D. W. Johnson, Jr., Phys. Rev. B **37**, 3745 (1988).

[2]R. J. Cava *et al.*, Nature (London) **332**, 814 (1988).

[3]D. W. Murphy, L. F. Schneemeyer, J. V. Waszczak, in *Chemistry of High-Temperature Superconductors II*, edited by D. L. Nelson and T. F. George (American Chemical Society, Washington, D.C., 1988).

[4]R. J. Cava *et al.*, Nature (London) **339**, 291 (1989).

[5]W. T. Fu *et al.*, Solid State Commun. **70**, 1117 (1989).
[6]K. Kourtakis and M. Robbins, Mater. Res. Bull. **24**, 1287 (1989).
[7]H. Uwe, J. Hirase, Y. Oiji, and T. Sakudo, in *Proceedings of the Tsukuba Seminar on High-T_c Superconductivity, Tsukuba, Japan, 1989,* edited by K. Masuda, T. Arai, I. Iguchi, and R. Yoshizaki (University of Tsukuba, Tsukuba, Japan, 1989).
[8]A. A. Verheijen, W. T. Fu, J. M. van Ruitenbeek, A. Smits, Q. Xu, and L. J. de Jongh, Solid State Commun. **71**, 573 (1989).
[9]Q. Xu, W. T. Fu, J. M. van Ruitenbeek, and L. J. de Jongh, Physica C **167**, 271 (1990).
[10]A. W. Sleight, J. L. Gillson, and P. E. Bierstedt, Solid State Commun. **17**, 27 (1975).
[11]S. N. Ruddlesden and P. Popper, Acta. Crystallogr. **10**, 538 (1957); **11**, 54 (1958).
[12]J. G. Bednorz and K. A. Müller, Z. Phys. B **64**, 189 (1986); J. G. Bednorz, M. Takashigi, and K. A. Müller, Europhys. Lett. **3**, 379 (1987).
[13]R. J. Cava, T. Siegrist, W. F. Peck, Jr., J. J. Krajewski, B. Batlogg, and J. Rosamilia, Phys. Rev. B **44**, 9746 (1991).
[14]L. F. Mattheiss, Phys. Rev. B **42**, 359 (1990).
[15]L. F. Mattheiss and D. R. Hamann, Phys. Rev. B **33**, 823 (1986).
[16]L. F. Mattheiss and D. R. Hamann, Phys. Rev. B **28**, 4227 (1983).
[17]L. F. Mattheiss and D. R. Hamann, Phys Rev. Lett. **60**, 2681 (1988).
[18]E. Wigner, Phys. Rev. **46**, 1002 (1934).
[19]Compared to earlier charge-density results for $BaBiO_3$ in Fig. 10 of Ref. 16, the diminished charge density near the Bi site in Fig. 3 is due to the fact that the Bi(5*d*) electrons are treated as core (rather than valence) electrons in the present calculation.
[20]M. Itoh, T. Sawada, R. Liang, H. Kawaji, and T. Nakamura, J. Solid State Chem. **87**, 245 (1990).
[21]M. Licheron, F. Gervais, J. Coutures, and J. Choisnet, Solid State Commun. **75**, 759 (1990).
[22]E. S. Hellman, E. H. Hartford, and E. M. Gyorgy, Appl. Phys. Lett. **58**, 1335 (1991).
[23]R. Weiss and R. Faivre, C. R. Acad. Sci. **248**, 106 (1959).

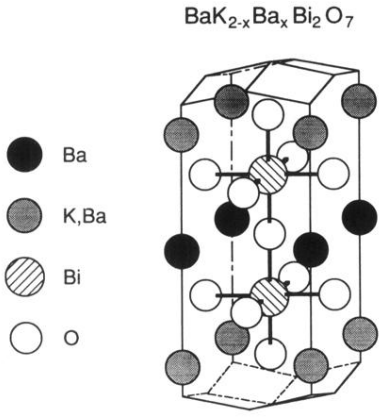

FIG. 1. Primitive body-centered-tetragonal unit cell for $BaK_{2-x}Ba_xBi_2O_7$. Oxygens in the Ba, Bi, and K-Ba planes are denoted O(1), O(2), and O(3), respectively.